ELSEVIER

www.elsevier.nl/locate/ica

Inorganica Chimica Acta 299 (2000) 155–163

Inorganica Chimica Acta

Synthesis and properties of $[Ru(tpy)(4,4'\text{-}X_2bpy)H]^+$ (tpy = 2,2′:6′,2″-terpyridine, bpy = 2,2′-bipyridine, X = H and MeO), and their reactions with CO_2

Hideo Konno [a], Atsuo Kobayashi [a], Kazuhiko Sakamoto [a], Florencia Fagalde [b], Néstor E. Katz [b], Hideki Saitoh [c], Osamu Ishitani [a,*]

[a] *Graduate School of Science and Engineering, Saitama University, 255 Shimo-Okubo, Urawa 338-8570, Japan*
[b] *Instituto de Química Física, Facultad de Bioquimica, Química y Farmacia, Universidad Nacional de Tucumán, Ayacucho 491, 4000 San Miguel de Tucumán, Argentina*
[c] *Faculty of Science, Saitama University, 255 Shimo-Okubo, Urawa 338-8570, Japan*

Received 8 June 1999; accepted 20 September 1999

Abstract

A novel type of hydrido complex $[Ru(tpy)(4,4'\text{-}X_2bpy)H]^+$ (X = H and MeO) was synthesized. The stronger hydridic character of the complexes compared with $[Ru(bpy)_2(L)H]^+$ type complexes (L = CO, PPh_3 and $AsPh_3$) was demonstrated by the relatively high chemical shifts of Ru–H in the ^1H NMR spectra and by higher reactivities with CO_2. The reactions of $[Ru(tpy)(4,4'\text{-}X_2bpy)H]^+$ with CO_2 occurred at second-order rate constants varying from (4.69 ± 0.02) to $(5.51 \pm 0.04) \times 10^{-3}$ M^{-1} s^{-1} depending on both solvent and X, giving the formato complexes $[Ru(tpy)(4,4'\text{-}X_2bpy)(OCHO)]^+$ quantitatively. The rate constant was increased with the increase of solvent acceptor number, and the reaction of $[Ru(tpy)\{4,4'\text{-}(MeO)_2bpy\}H]^+$ with CO_2 was found to be 3.6 times faster than that of $[Ru(tpy)(bpy)H]^+$. These results suggest that nucleophilic attack of the hydride ligand to the carbon atom of CO_2 is the rate determining step for the formation of the formato complex. The structure of the formato complex $[Ru(tpy)(bpy)(OCHO)](PF_6)$ was determined by X-ray crystallographic analysis.

Keywords: Crystal structures; Ruthenium complexes; Hydrido complexes; Formato complexes

1. Introduction

Polypyridine metal hydrides have been of interest for many years because they often play important roles as intermediates in many catalytic redox reactions, such as CO_2 reduction [1–11], hydrogen evolution [12] and water–gas-shift reactions [13,14]. The insertion of CO_2 into a metal–hydride bond and its reverse reaction are key processes in the reduction of CO_2 and water–gas-shift reactions [15–19].

Ruthenium polypyridine complexes have been often used as photocatalysts [6,10,20–24] and electrocatalysts [1,2,25–28]. In a previous paper [22], we reported that $[Ru(tpy)(bpy)(py)]^{2+}$ (tpy = 2,2′:6′,2″-terpyridine, bpy = 2,2′-bipyridine, py = pyridine) photocatalyzes the selective hydride reduction of an $NAD(P)^+$ model compound via the hydrido complex intermediate, $[Ru(tpy)(bpy)H]^+$ [22]. In the electrochemical six-electron reduction of CO_2 to methanol using $[Ru(tpy)(bpy)(CO)]^{2+}$ as an electrocatalyst [27], it appears that $[Ru(tpy)(bpy)H]^+$ might be also generated to play important roles, but no information has been given concerning its role. Although ruthenium hydrido complexes have been assumed to play important roles in multi-electron (or hydride) reduction reactions catalyzed by ruthenium polypyridine complexes, only a few polypyridine ruthenium hydrido complexes have been isolated [12,29,30] mainly because of their instability, and the isolated hydrido complexes reveal little reactivity towards electrophilic reactants such as CO_2 and

* Corresponding author. Tel.: +81-488-583 733; fax: +81-488-583 818.
E-mail address: ishitani@apc.saitama-u.ac.jp (O. Ishitani)

0020-1693/00/$ - see front matter
PII: S0020-1693(99)00488-0

water because they have a strong π-acidic ligand, i.e. CO, PPh_3 or $AsPh_3$.

We wish to report here the synthesis of new hydrido complexes $[Ru(tpy)(4,4'\text{-}X_2bpy)H]^+$ (**1**: X = H and **2**: MeO) and their chemical behavior associated with the reactions with CO_2.

2. Experimental

2.1. General procedures

The redox potentials of the complexes were measured in an acetonitrile solution containing tetra-n-butylammonium tetrafluoroborate (0.1 M) as the supporting electrolyte by cyclic voltammetric techniques using an ALS/CHI CHI-620 electrochemical analyzer, with a Pt disk working electrode, a $Ag/AgNO_3$ (0.01 M) reference electrode and a Pt counter electrode. The supporting electrolyte was dried in vacuo at 100°C for 3 days prior to use. UV–Vis and IR absorption spectra were recorded on Photal MCPD-1000 and Jeol JIR-6500 spectrometers, respectively. ^1H NMR (500 MHz) spectra were recorded on a Jeol 500 NMR spectrometer at 25°C. Electrospray ionization (ESI) mass spectra were measured using a Hitachi M-1200 mass spectrometer with a M-1206 ES probe. The positive ion ESI MS spectra were measured with a 10 V drift voltage by a procedure reported elsewhere [31].

2.2. Materials

Acetonitrile was distilled over P_2O_5 three times and then over CaH_2 just before use. *N*,*N*-Dimethylformamide (DMF) was dried over 4 Å molecular sieves and distilled at reduced pressure ($\sim$20 Torr) before use. Methanol and ethanol were distilled over the corresponding magnesium alcoxides. Acetone was dried over 4 Å molecular sieves for several days and distilled under an Ar atmosphere. The compound $RuCl_3 \cdot 3H_2O$ was kindly supplied by Kojima Chemical Co.

2.3. Synthesis

2.3.1. $[Ru(tpy)(bpy)H](PF_6) \cdot 0.5H_2O$ (1)

To a deaerated solution of $[Ru(tpy)(bpy)Cl](PF_6)$ (263.0 mg) [32] in ethanol (43 ml)–water (20 ml) was added dropwise an aqueous solution of $NaBH_4$ (279.0 mg), and then the mixture was refluxed for 20 min under an Ar atmosphere. After addition of saturated aqueous solution of KPF_6 (1 ml) to the mixture at room temperature (r.t.), the solution was evaporated to $\sim$10 ml under reduced pressure at r.t. to precipitate black crystals of **1**, which were collected by filtration, washed with cold water, and then dried in vacuo. Isolated yield: 70%. ^1H NMR (DMSO-d_6): δ 9.67 (d, $J = 5.5$ Hz, 1H, H-1), 8.85 (d, $J = 8.0$ Hz, 1H, H-4), 8.66 (d, $J = 8.0$ Hz, 2H, H-17, 19), 8.64 (d, $J = 8.0$ Hz, 1H, H-7), 8.60 (d, $J = 8.0$ Hz, 2H, H-14, 22), 8.18 (dd, $J = 8.0$, 7.7 Hz, 1H, H-3), 7.94 (t, $J = 8.0$ Hz, 1H, H-18), 7.87 (dd, $J = 8.0$, 7.7 Hz, 2H, H-13, 23), 7.82 (dd, $J = 8.0$, 7.7 Hz, 1H, H-8), 7.79 (dd, $J = 7.7$, 5.5 Hz, 1H, H-2), 7.76 (d, $J = 5.5$ Hz, 2H, H-11, 25), 7.29 (dd, $J = 7.7$, 5.5 Hz, 2H, H-12, 24), 7.11 (dd, $J = 7.7$, 5.5 Hz, 1H, H-9), 7.03 (d, $J = 5.5$ Hz, 1H, H-10), −14.64 (s, 1H, Ru–H). IR (KBr): ν(Ru–H) = 1860 cm^{-1}. *Anal.* Calc. for $C_{25}H_{21}F_6N_5O_{0.5}PRu$: C, 46.55; H, 3.20; N, 10.86. Found: C, 46.38; H, 3.12; N, 10.66%. Electronic absorption spectrum (CH_3CN): λ_{max}, nm (ε, M^{-1} cm^{-1}) 534 (11 000), 384 (8600), 319 (25 000), 297 (20 000). ESI MS: m/z 492 (main peak, M^+, where $M = [Ru(tpy)(bpy)H]$), 245 ($\{M^+ - H^-\}^{2+}$).

2.3.2. $[Ru(tpy)\{4,4'\text{-}(MeO)_2bpy\}Cl](PF_6)$

This complex was synthesized using a procedure analogous to the reported method for $[Ru(tpy)(bpy)Cl](PF_6)$, except that 4,4′-dimethoxy-2,2′-bipyridine [33] was used instead of bpy. Isolated yield: 60%.

2.3.3. $[Ru(tpy)\{4,4'\text{-}(MeO)_2bpy\}H](PF_6) \cdot 0.5H_2O$ (2)

Complex **2** was synthesized using a procedure analogous to that given for **1**, except that $[Ru(tpy)\{4,4'\text{-}(MeO)_2bpy\}Cl](PF_6)$ was used as the starting material. Column chromatography using aluminum oxide and 3:1 CH_3CN/toluene as eluent can be used for purification of **2** if necessary. The chromatographic purification should be carried out under an Ar atmosphere and reduced lighting. The first blue–violet band was collected and the eluent was evaporated under reduced pressure to yield black crystals of **2**. These crystals were dried in vacuo. The typical yields were 70 and 50% before and after the chromatographic purification, respectively. ^1H NMR (CD_3CN): δ 9.45 (d, $J = 6.5$ Hz, 1H, H-1), 8.32 (d, $J = 7.6$ Hz, 2H, H-17, 19), 8.28 (d, $J = 7.6$ Hz, 2H, H-14, 22), 8.09 (s, 1H, H-4), 7.91 (d, $J = 5.5$ Hz, 2H, H-11, 25), 7.85 (s, 1H, H-7), 7.79 (t, $J = 7.6$ Hz, 1H, H-18), 7.78 (t, $J = 7.6$ Hz, 2H, H-13, 23), 7.32 (d, $J = 6.5$ Hz, 1H, H-2), 7.20 (dd, $J = 7.6$, 5.5 Hz, 2H, H-12, 24), 6.78 (d, $J = 6.1$ Hz, 1H, H-10), 6.53 (d, $J = 6.1$ Hz, 1H, H-9), 4.13 (s, 3H, MeO), 3.80 (s, 3H, MeO), −15.52 (s, 1H, Ru–H). IR (KBr): ν(Ru–H) = 1863 cm^{-1}. *Anal.* Calc. for $C_{27}H_{25}F_6N_5O_{2.5}PRu$: C, 45.96; H, 3.57; N, 9.93. Found: C, 46.08; H, 3.34; N, 9.66%.

2.4. Reaction of the hydrido complexes with CO_2

After bubbling of CO_2 into various solutions of **1** or **2** for several minutes, the solutions were directly subjected to ESI MS analysis. For all the solutions, the parent-ion peaks corresponding to the formato complexes $[Ru(tpy)(4,4'\text{-}X_2bpy)(OCHO)]^+$ (**3**: X = H, **4**:

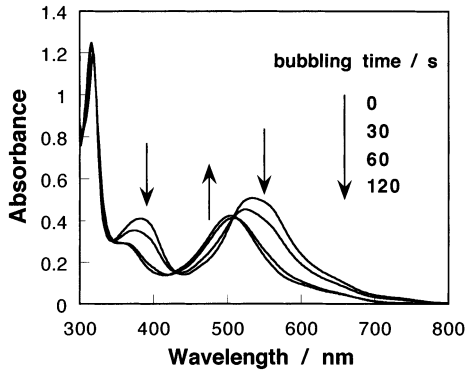

Fig. 1. UV–Vis absorption spectral changes in an acetonitrile solution containing **1** (4.8×10^{-2} mM) during CO_2 bubbling.

X = MeO) were observed as the main peak. The progress of the reactions of **1** and **2** with CO_2 was followed by the UV–Vis absorption spectra. Fig. 1 shows such spectral changes for an acetonitrile solution of **1**; CO_2 bubbling caused a rapid hypsochromic shift of the absorption maximum from 534 nm for the metal-to-ligand charge transfer (MLCT) transition of **1** to the final one at 504 nm, accompanied by a set of isosbestic points between 300 and 800 nm. The final spectrum was identical to that of the formato complex. Similar spectral changes were observed in all the solvents and for the both hydrido complexes.

2.5. Isolation of [Ru(tpy)(bpy)(OCHO)](PF$_6$)·0.5H$_2$O (3)

A 300 ml methanolic solution containing **1** (51.8 mg) was bubbled with CO_2 at r.t. for about 30 min. Evaporation of the solution under reduced pressure at ambient temperature gave black crystals of **3**. Isolated yield: 84%. ^{1}H NMR (DMSO-d$_6$): δ 9.64 (d, $J = 5.6$ Hz, 1H, H-1), 8.90 (d, $J = 8.2$ Hz, 1H, H-4), 8.76 (d, $J = 8.0$ Hz, 2H, H-17, 19), 8.64 (d, $J = 7.9$ Hz, 2H, H-14, 22), 8.60 (d, $J = 7.9$ Hz, 1H, H-7), 8.36 (dd, $J = 8.2$, 7.3 Hz, 1H, H-3), 8.18 (t, $J = 8.0$ Hz, 1H, H-18), 8.10 (dd, $J = 7.3$, 5.6 Hz, 1H, H-2), 7.97 (dd, $J = 7.9$, 7.5 Hz, 2H, H-13, 23), 7.73 (dd, $J = 7.9$, 7.3 Hz, 1H, H-8), 7.63 (d, $J = 5.5$ Hz, 2H, H-11, 25), 7.57 (s, 1H, OCHO), 7.36 (dd, $J = 7.5$, 5.5 Hz, 2H, H-12, 24), 7.13 (d, $J = 5.8$ Hz, 1H, H-10), 7.06 (dd, $J = 7.3$, 5.8 Hz, 1H, H-9). IR (KBr): $\nu(OCO)_{asym} = 1618$ cm^{-1}, $\nu(OCO)_{sym} = 1318$ cm^{-1}. *Anal.* Calc. for $C_{26}H_{21}F_6N_5O_{2.5}PRu$: C, 45.29; H, 3.07; N, 10.16. Found: C, 45.38; H, 3.01; N, 10.54%. Electronic absorption spectrum (CH_3CN): λ_{max}, nm (ε, M^{-1} cm^{-1}) 504 (9000), 316 (30 000), 292 (32 000). ESI MS: m/z 535 (main peak, M^+, where M = [Ru(tpy)(bpy)(OCHO)]), 245 ($\{M^+ - (OCHO)^-\}^{2+}$).

Table 1
Crystallographic data for [Ru(tpy)(bpy)(OCHO)](PF$_6$)·3H$_2$O

Chemical formula	$C_{26}H_{26}N_5F_6PRu$
Formula weight	734.59
Sample size (mm)	$0.40 \times 0.20 \times 0.20$
Color and shape	black prism
Crystal system	monoclinic
Space group	$P2_1/n$ (no. 14)
a (Å)	15.959(6)
b (Å)	13.268(5)
c (Å)	14.259(4)
β (°)	99.47(3)
V (Å^3)	2978.1(17)
Z	4
T (K)	295
D_{calc} (g cm^{-3})	1.638
Linear absorption coefficient μ (cm^{-1})	6.479
$F(000)$	1480
R [a]	0.078
wR [b]	0.067
S [c]	2.547

[a] $R = \Sigma(||F_o| - |F_c||)/\Sigma|F_o|$.
[b] $wR = [\Sigma w(|F_o| - |F_c|)^2/\Sigma w|F_o|^2]^{1/2}$.
[c] $S = [\Sigma w(|F_o| - |F_c|)^2/(m-n)]^{1/2}$.

2.6. Crystal structure determination of 3

All X-ray data were obtained on a Mac Science MXC18K four-circle diffractometer using graphite-monochromated Mo Kα ($\lambda = 0.71073$ Å) radiation. The unit cell dimensions were determined from 22 reflections in the range of $26° < 2\theta < 35°$. The crystallographic data are given in Table 1. A total of 11 291 diffraction–intensity data were collected using the 2θ–θ scan over all the 2θ range 3.0–50.0°. Three standard reflections were measured at an interval of 100 reflections. The intensity data were corrected for Lorentz and polarization effects. The absorption correction was not applied. The space group $P2_1/n$ was selected based on the systematic absence of the reflections. The crystal structure was solved by the direct method using the SIR-92 program [34]. All computations were carried out using the CRYSTAN-GM program system [35]. Of the 5235 unique reflections ($R_{int} = 0.10$), over the index ranges $18 > h > 0$, $15 > k > 0$ and $16 > l > -16$, the 3136 reflections with criterion $I_o > 1.5\sigma(I_o)$ over the index ranges were used in the full-matrix least-squares refinements based on minimization of the function $\Sigma w(|F_o| - |F_c|)^2$. The weighting scheme was $w^{-1} = \sigma^2(F_o) + 0.0004|F_o|^2$. The atomic and anomalous scattering factors were taken from the literature [36]. All non-hydrogen atoms were refined anisotropically. Hydrogen atoms, except for H(26) at the formate moiety, were assigned by calculation and their parameters were restrained for the C–H length 0.96 Å and fixed the thermal parameters U_{iso} 0.07 Å^2. The H(26) atom was located in difference syntheses and refined isotropically. No secondary extinction corrections were applied. The number of the refined parameters was 401. The final R and wR factors were 0.078 and 0.067, respectively. The goodness-of-fit (S) was 2.547. The largest Δ/ρ value was 0.0002. The largest peak and hole differences were 0.76 and -0.83 e Å^{-3}, respectively.

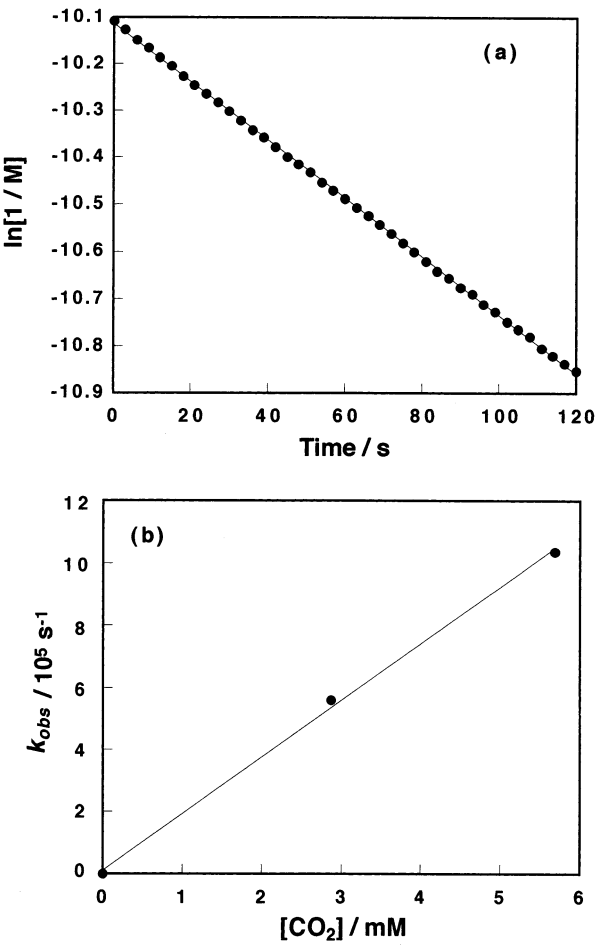

Fig. 2. Reaction of **1** with excess CO_2 in an acetonitrile solution: (a) decay of **1**, and (b) relationship between observed pseudo-first-order rate constants (k_{obs}) and concentration of CO_2.

2.7. Measurement of CO_2 concentrations in various solvents

Saturated concentrations of CO_2 in various solvents were obtained by the titration method reported by Fujita et al. [37,38]. A 5 ml solvent in a reaction vessel (8.3 ml capacity) was gently bubbled with CO_2 for 20 min and sealed with a rubber septum (Aldrich) to give the CO_2-saturated solution. A 1 ml portion of the solution was transferred into a standardized 0.025 M $Ba(OH)_2$ solution (25 ml) to precipitate $BaCO_3$. The solution was then back-titrated with a standardized 0.1 M HCl solution using *m*-cresol purple as an indicator. The titration experiments were repeated 2–3 times for each solvent, and the concentrations of CO_2 were reproduced within $\pm 7\%$.

2.8. Kinetic studies

A 5 ml solution containing **1** or **2** (1.8×10^{-4}–1.8×10^{-5} mM) in a quartz cubic cell (8.3 ml) was gently bubbled with Ar for 20 min and then sealed with a rubber septum. A 20–100 μl CO_2-saturated solution was added into the cell using a gas-tight syringe. The UV–Vis absorption spectra were measured every 10–180 s. The absorption at 550 or 560 nm was monitored for the determination of concentration of the hydrido and formato complexes using the following ε values: ε at 550 nm, M^{-1} cm^{-1} (solvent); **1** = 11 000 (DMF), 8900 (acetone), 7900 (EtOH), 7000 (MeOH), **3** = 3900 (DMF), 3600 (acetone), 4200 (EtOH), 3400 (MeOH), ε at 560 nm, M^{-1} cm^{-1} (solvent); **1** = 10 000 (CH_3CN), **3** = 3900 (CH_3CN), **2** = 6500 (CH_3CN), **4** = 3500 (CH_3CN). Fig. 2 shows a time-conversion curve of **1** for an acetonitrile solution containing 5.7 mM CO_2 (a) and the relationship between the pseudo-first-order rate constants (k_{obs}) calculated from the time-conversion curves for **1** and the concentration of CO_2 (b).

3. Results and discussion

3.1. Properties of *1* and *2*

To the best of our knowledge, the first reported polypyridine ruthenium hydrido complex is $[Ru(bpy)_2(CO)H]^+$ [12]. This complex is relatively stable and does not react with CO_2 at ambient temperature [10], probably because of the low nucleophilic character of the hydride ligand due to the strong π-backbonding of Ru(II) to the CO ligand. Similar hydrido complexes with other π-accepting ligands, i.e. $[Ru(bpy)_2(PPh_3)H]^+$ and $[Ru(bpy)_2(AsPh_3)H]^+$, are also stable enough to be isolated [29], while $[Ru(bpy)_2(py)H]^+$ has not been isolated by similar methods because of its instability arising from the much weaker π-accepting ability of the pyridine ligand compared with the CO, PPh_3 and $AsPh_3$ ligands. In the present work, we have succeeded in the isolation of **1** and **2** by manipulation under deaerated and dimmed light conditions. It should be noted that **1** and **2** remain unchanged in the solid state for several months by keeping in a refrigerator, and even in degassed solutions such as methanol and ethanol for at least several hours at r.t. In aerated solutions, on the other hand, it was found that these complexes are changed mainly by the reaction with atmospheric CO_2 leading to the formation of the formato complexes (vide infra). It is of interest to note that **1** is stable enough to be isolated unlike $[Ru(bpy)_2(py)H]^+$. Although the reason is still in question, the terpyridine ligand might cause some strain in the metal coordination to influence the properties of the Ru–H bond.

In the ^1H NMR spectra of **2**, the signal of Ru–H appears at a higher field (-15.52 ppm) compared to **1** (-14.69 ppm), clearly indicating that **2** has a stronger hydricity, i.e. higher hydride donating ability, than **1**,

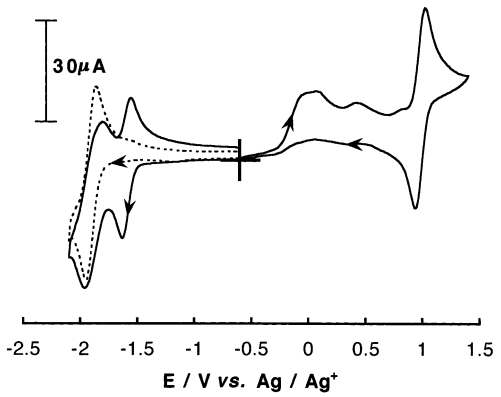

Fig. 3. Cyclic voltammograms of **1** (3.4 mM) in an acetonitrile solution containing $^{n}Bu_4NBF_4$ (0.1 M) under an Ar atmosphere at a scan rate of 200 mV s^{-1}: (solid line) initial processes are anodic, and (dotted line) initial processes are cathodic.

probably because of the stronger electrodonating ability of $(MeO)_2$bpy compared with bpy.

Fig. 3 illustrates the cyclic voltammograms of **1** in an acetonitrile solution in a potential range of 1.4 to −2.1 V. The cathodic quasi-reversible wave shown with a dotted line is attributable to the tpy-based reduction. The reduction potential of **1** is more negative than those of other $[Ru(tpy)(bpy)L']^+$ type complexes ($L' = Cl^-$ and HCO_2^-), as shown in Table 2, probably arising from the strong electron-donating ability of the hydride ligand. As shown by a solid line in Fig. 3, on the other hand, the anodic oxidation of **1** irreversibly occurred to give the acetonitrile complex $[Ru(tpy)(bpy)(CH_3CN)]^{2+}$, whose redox potentials are known to appear at 0.99 and −1.59 V versus $Ag/AgNO_3$ [32]. The electrochemical formation of $[Ru(tpy)(bpy)(CH_3CN)]^{2+}$ should proceed via a sequential loss of two electrons and a proton from **1** followed by the coordination of a solvent molecule (Eq. (1)).

Table 2
Electrochemical data of $[Ru(tpy)(bpy)L']^{n+}$ measured in an CH_3CN solution containing 0.1 M $^{n}Bu_4NBF_4$

L′	n	$E_{1/2}$ (V vs. $Ag/AgNO_3$) [a]	
		Oxidation	Reduction
H^- [b]	1	−0.12 [c]	−1.91 (90), −2.17 (80) [d]
HCO_2^- [b]	1	0.47 (70)	−1.71 (80), −1.92 [c]
Cl^- [e]	1	0.49 (80)	−1.75 (90), −1.94 [c]
py [e]	2	0.92 (80)	−1.56 (70), −1.89 (80)
CO [f]	2		−1.35, −1.69 [c]

[a] Pt-disk working (1.6 mm i.d.) and Pt-wire counter electrodes were used. Values in parentheses are peak-to-peak separations in mV.
[b] Scan rate 0.2 V s^{-1}.
[c] Irreversible peak.
[d] This quasi-reversible wave is not shown in Fig. 1.
[e] Scan rate 1.0 V s^{-1}.
[f] From Ref. [27]. The oxidation wave has not been reported.

$$[Ru(tpy)(bpy)H]^+ \xrightarrow[CH_3CN]{-2\,e^-} [Ru(tpy)(bpy)(CH_3CN)]^{2+} + H^+ \quad (1)$$

3.2. Reactions of *1* and *2* with CO_2

Upon bubbling of CO_2 into a methanolic solution of **1** at 25°C for 30 min, black crystals were obtained after evaporation of the solvent. The ESI MS spectrum of the product shows a parent peak at $m/z = 535$, demonstrating that the product is an adduct of **1** with CO_2, presumably formed by the reductive fixation of CO_2 into the Ru–H bond. The adduct shows a singlet at 7.57 ppm in the ^1H NMR spectrum, which remained unchanged upon addition of D_2O. Therefore, CO_2 should be fixed as the metal-formate bonding but not as the metallo carboxylic acid form. Moreover, the IR absorptions of the adduct at 1318 and 1618 cm^{-1} can be assigned as the symmetric and asymmetric stretching vibrations of the formate ligand, respectively. The difference of the bands (300 cm^{-1}) is in accord with the monodentate coordination of the formate anion, while the η^2-coordination would give a difference of less than 201 cm^{-1} [39]. These spectral data clearly indicate that the adduct is the formato complex **3** (Eq. (2)). The structure of **3** was explicitly determined by X-ray crystallography (vide infra).

$$[Ru(tpy)(bpy)H]^+ + CO_2 \rightarrow [Ru(tpy)(bpy)(OCHO)]^+ \quad (2)$$

The adduct **3** was isolated in 84% yield based on **1** used. Moreover, the UV–Vis absorption changes of an acetonitrile solution of **1** caused by CO_2 bubbling (Fig. 1) are accompanied by a set of isosbestic points, and the final spectrum is essentially identical with that of **3**. This clearly indicates that the reductive fixation of CO_2 quantitatively proceeds. Therefore, kinetic studies on the reaction could be easily performed by in situ measurements of UV–Vis spectral changes occurring after addition of a fixed amount of CO_2-saturated solution into the solution of **1**. Fig. 2(a) shows a pseudo-first-order kinetic plot for the disappearance of **1** in the presence of excess CO_2, from which the apparent first order rate constant (k_{obs}) was obtained. From a linear plot of k_{obs} versus CO_2 concentration (Fig. 2(b)), the second-order rate constant (k_2) of the reaction was determined as 1.82×10^{-2} M^{-1} s^{-1} in CH_3CN using Eq. (3).

$$-\frac{d[\mathbf{1}]}{dt} = k_2[\mathbf{1}][CO_2] \quad (3)$$

Similarly, the k_2 values for various solutions of **1** were obtained, since the reaction of Eq. (2) in other solvents again proceeded in a quantitative manner. As shown in Table 3, the second-order reaction rate constants dramatically vary by three orders of magnitude.

Table 3
Second-order rate constants (k_2) of the reaction between the hydride complex and CO_2 in various solvents, and the parameters of the solvents

Complex	Solvent	k_2 (M^{-1} s^{-1})	$[CO_2]$ [a] (M)	AN [b]	DN [c]	D_s [d]
1	MeOH	4.69 ± 0.02	0.14	41.3	19.1	32.6
1	EtOH	$(3.64 \pm 0.11) \times 10^{-1}$	0.10	37.1	20.0	24.3
1	CH_3CN	$(1.82 \pm 0.07) \times 10^{-2}$	0.29	18.9	14.1	36.1
2	CH_3CN	$(6.39 \pm 0.07) \times 10^{-2}$	0.29	18.9	14.1	36.1
1	DMF	$(1.75 \pm 0.28) \times 10^{-2}$	0.20	16.0	26.6	36.7
1	acetone	$(5.51 \pm 0.04) \times 10^{-3}$	0.29	12.5	17.0	20.7

[a] Saturated concentration of CO_2.
[b] Acceptor number of solvent [40].
[c] Donor number of solvent [41].
[d] Static dielectric constant of solvent [9,42].

We found that $\ln(k_2)$ values are in a good linear relationship with the acceptor number (AN) of the solvents [40], as shown in Fig. 4, while no linear correlation was observed between k_2 and the donor number (DN) [41]. Moreover, no correlation can be seen between k_2 and the static dielectric constants (D_s) of the solvents (Table 3). This does not agree with the observation reported for the reaction of rhenium polypyridine hydrido complexes with CO_2 [9], the second-order rate constant of which was reported to increase with D_s.

These kinetic results are certainly of mechanistic importance associated with the intermediates and transition states for the CO_2 fixation. Since the second-order kinetics of the CO_2 fixation should eliminate the possible participation of any dissociative mechanism, we considered the following four possible transition states on this reaction (Scheme 1); (a) the hydride ligand interacts with the carbon center of CO_2, ((b) and (c)) the oxygen atom (terminus) or the C=O bond of CO_2 interacts with the ruthenium center, and (d) the Ru–H bond interacts with the C=O bond of CO_2 to form a four-membered cyclic transition state. Since AN and DN are known to relate with the Lewis acidity and basicity of solvent respectively, the linear correlation of $\ln(k_2)$ with AN strongly suggests that the Lewis-acid character of the solvents should exert important effects on the transition state of the CO_2 fixation. A reasonable

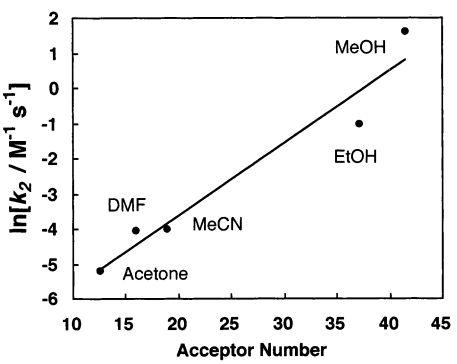

Fig. 4. Relationship between second-order rate constants (k_2) measured in various solvents and acceptor numbers (AN) of the solvents.

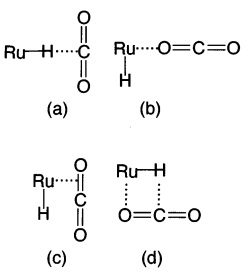

Scheme 1.

speculation is that the Lewis acid center of solvent molecules might interact with the oxygen atom of CO_2 to activate the carbon atom of CO_2 towards the nucleophilic attack of the hydride ligand ((a) or (d)). Alternatively, Lewis-acid interactions of solvent molecules with the ligands of the hydrido complex would occur to cause a decrease of electron density on the Ru center. If this is the case, the Ru center would approach the oxygen terminus of CO_2 in the transition state ((b)–(d)).

For mechanistic elucidation, it is of significance to consider the relatively high reactivity of **1** with CO_2 versus the unreactive nature of $[Ru(bpy)_2(L)H]^+$ (L = CO [10], PPh_3 and $AsPh_3$ [43]). This crucial reactivity difference can be easily related to the much stronger π-acidities of L in $[Ru(bpy)_2(L)H]^+$ compared with the pyridine part of the tpy ligand of **1**. In the former, therefore, the hydridic nature of Ru–H should be lower than that of **1**. The higher hydricity of **1** is also supported by ^1H NMR chemical shift of **1** which is higher by ~ 3 ppm in field than that of $[Ru(bpy)_2(L)H]^+$.[1] On

[1] Although chemical shifts for metal hydrides depend on various factors, we can safely use the ^1H NMR results of **1** and $[Ru(bpy)_2(L)H]^+$ for the comparison of their hydricities, because their structures are very similar to each other. The difference of the Ru–H chemical shifts would be attributed to deshielding effects of the ligands coordinating at the *cis* position of the hydride. However, this is clearly not the case, because the deshielding effects due to the three pyridine rings of the tpy ligand of **1** are undoubtedly stronger than the combined effects of the bpy and L ligands in $[Ru(bpy)_2(L)H]^+$ (the ligand L coordinates at the *cis* position of the hydride ligand).

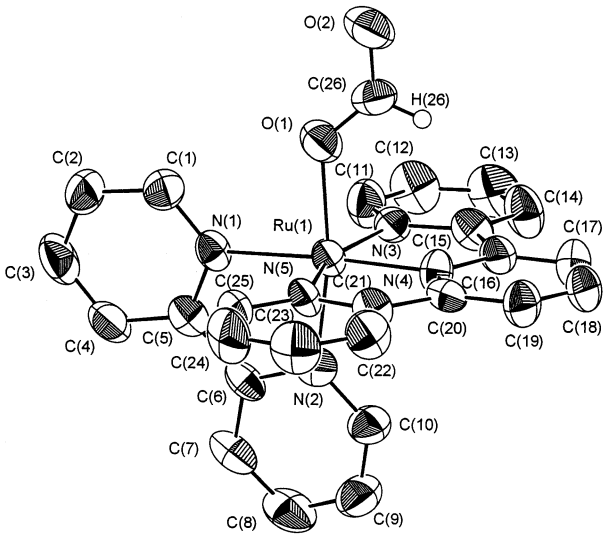

Fig. 5. ORTEP drawing (50% probability thermal ellipsoids) and labeling scheme for the atoms of the cation of **3**.

the basis of this argument, it can be easily understood why **2** is 3.6 times more reactive with CO_2 than **1** (Table 3), since the electron-donating ability of the methoxy groups of the $(MeO)_2$bpy ligand can induce an increase of electron density on the ruthenium center to enhance the hydridic character of Ru–H for **2** [9,44].

These results strongly suggest that the nucleophilic attack of the hydride ligand to the carbon atom of CO_2 is the rate determining step in the formation of the formato complex, while electrophilic interactions of the ruthenium center with the oxygen terminus of CO_2 should be less important in the transition state, if any. Therefore, the preferred transition state should be (a) and/or (d) in Scheme 1.

Table 4
Selected bond lengths (Å) and angles (°) for [Ru(tpy)(bpy)(OCHO)]-$(PF_6)\cdot 3H_2O$

Bond lengths			
Ru–O(1)	2.094(11)	Ru–N(1)	2.080(11)
Ru–N(2)	2.011(12)	Ru–N(3)	2.083(13)
Ru–N(4)	1.975(12)	Ru–N(5)	2.061(12)
O(1)–C(26)	1.21(3)	O(2)–C(26)	1.25(3)
C(26)–H(26)	0.90(17)		
Bond angles			
Ru–O(1)–C(26)	128.3(11)	O(1)–C(26)–H(26)	114.9(107)
O(1)–C(26)–O(2)	127.9(18)	O(2)–C(26)–H(26)	117.0(108)
N(1)–Ru–N(2)	79.4(5)	N(2)–Ru–O(1)	169.9(5)
N(3)–Ru–N(4)	79.5(5)	N(3)–Ru–O(1)	92.9(5)
N(4)–Ru–N(5)	80.4(5)	N(4)–Ru–O(1)	93.0(5)
N(1)–Ru–O(1)	90.5(5)	N(5)–Ru–O(1)	89.0(5)

3.3. Crystal structure and electrochemical properties of **3**

Although formato transition metal complexes have been supposed as important intermediates in various catalytic reactions [45], relatively few η^1-formate complexes have been structurally characterized to date [46–54]. We were able to obtain single crystals of **3**, suitable for X-ray crystallographic analysis. The ORTEP structure is shown in Fig. 5, and selective bond lengths and angles are summarized in Table 4. The result clearly shows that the formate is bonded to the ruthenium center on the oxygen atom O(1) as a η^1-ligand. Its bond length is 2.094(11) Å. The bond length between the carbon C(26) and the hydrogen H(26) atom, which could be refined anisotropically, is 0.90(17) Å, and the angle O(1)–C(26)–O(2) is 128.3(11)°. Interestingly, the C(26)–O(1) 'single bond' and the C(26)–O(2) 'double bond' have very similar bond lengths (1.22(3) and 1.26(3) Å).[2] A similar observation was reported for *trans*-$Ru(dmpe)_2(OCHO)H$ ($dmpe = Me_2PCH_2CH_2PMe_2$) [47]. Since typical lengths of C–O and C=O bonds are 1.43 Å and 1.23 Å respectively, it is surprising that the two carbon–oxygen bonds of the formate ligand in **3** are similar to typical C=O double bonds in length but significantly shorter than a typical C–O single bond.

In order to obtain structural implications for **3**, we compared the X-ray crystallographic data of **3** with those reported for several $[Ru(tpy)(bpy)L']^{n+}$ type complexes ($n = 1$ or 2; $L' = CO$ [27], I^- [55], CH_3CN [32], pyridine [56] and its derivatives [32,57]). The Ru–N(2) bond for the one pyridine ring of the bpy ligand *trans* to the formate ligand is 2.006(12) Å, slightly shorter than the Ru–N(2) bond for the other pyridine ring (2.088(11) Å) and also than the Ru–N bond for the bpy ligand in $[Ru(tpy)(bpy)L']^{n+}$ type complexes (2.036(6) Å for $n = 1$: $L' = I^-$; 2.040(9)–2.093(3) Å for $n = 2$: $L' = CO$ [27], CH_3CN [32], pyridine [56] and its derivatives [32,57]). These results might be explained by the strong interaction of the non bonding p-orbital on O(1) and the d-orbital of the ruthenium(II), that is to say, the formate ligand probably works not only as a σ-base but also as a π-base. Such a interaction can enrich π-back donation from the ruthenium to the pyridine ring of the bpy ligand *trans* to the formate ligand to shorten the bond length between the ruthenium and N(2).

The cyclic voltammogram of **3** shows anodic and cathodic reversible redox waves, which can be attributed to tpy-based reduction ($tpy/tpy^{-\bullet}$) and metal-based oxidation ($Ru^{II/III}$), respectively. Table 2 shows

[2] There is no indication of packing effects, which should influence the bond lengths around the ruthenium(II) of **3**.

the electrochemical data of **3**, together with those of $[Ru(tpy)(bpy)L']^{n+}$ type complexes in an acetonitrile solution. The redox potentials of **3** are similar to those of $L' = Cl^-$, which is a typical π-base ligand.

4. Conclusions

The new hydrido complexes $[Ru(tpy)(4,4'\text{-}X_2bpy)H]^+$ (X = H and MeO) have been synthesized in reasonable yields. The stronger hydridic characters of the complexes compared with $[Ru(bpy)_2(L)H]^+$ type complexes (L = CO, PPh_3 and $AsPh_3$) were demonstrated by the higher chemical shifts of Ru–H in the ^1H NMR spectra and by their higher reactivities with CO_2. The hydrido complexes react with CO_2 to give the formato complexes $[Ru(tpy)(bpy)(OCHO)]^+$, quantitatively, the structure of which has been determined by X-ray crystallographic analysis. Experimental results show that nucleophilic attack of the hydride ligand to the carbon atom of CO_2 is the rate-determining step.

5. Supplementary material

Further atomic parameters, bond lengths, bond angles and thermal parameters have been deposited at the Cambridge Crystallographic Data Centre, CCDC No. 135211.

Acknowledgements

We acknowledge helpful discussion with Dr Kazuhide Koike, Dr Hisao Hori (NIRE), Dr Jeremy R. Westwell (Unilever Research) and Dr Chongjin Pac (Kawamura Institute of Chemical Research). We also thank the Kojima Chemical Co. for the gift of $RuCl_3 \cdot 3H_2O$. This work has been supported by RITE (Research Institute of Innovative Technology for the Earth). F.F. and N.E.K. are Members of the Research Career of CONICET (Consejo Nacional de Investigaciones Cientificas y Técnicas, Argentina). We thank CONICET and UNT (Universidad Nacional de Tucumán, Argentina) for financial help to N.E.K.

References

[1] K. Tanaka, Bull. Chem. Soc. Jpn. 71 (1998) 17.
[2] B.P. Sullivan, K. Krist, H.E. Guard (Eds.), Electrochemical and Electrocatalytic Reactions of Carbon Dioxide, Elsevier, Amsterdam, 1993.
[3] H. Hori, F.P.A. Johnson, K. Koike, K. Takeuchi, T. Ibusuki, O. Ishitani, J. Chem. Soc., Dalton Trans. (1997) 1019.
[4] M.R.M. Bruce, E. Megehee, B.P. Sullivan, H.H. Thorp, T.R. O'Toole, A. Downard, J.R. Pugh, T.J. Meyer, Inorg. Chem. 31 (1992) 4864.
[5] J.R. Pugh, M.R. Bruce, B.P. Sullivan, T.J. Meyer, Inorg. Chem. 30 (1991) 86.
[6] J.-M. Lehn, R. Ziessel, J. Organomet. Chem. 382 (1990) 157.
[7] M.R.M. Bruce, E. Megehee, B.P. Sullivan, H. Thorp, T.R. O'Toole, A. Downard, T.J. Meyer, Organometallics 7 (1988) 238.
[8] J. Hawecker, J.-M. Lehn, R. Ziessel, Helv. Chim. Acta 69 (1986) 1990.
[9] B.P. Sullivan, T.J. Meyer, Organometallics 5 (1986) 1500.
[10] J. Hawecker, J.-M. Lehn, R. Ziessel, J. Chem. Soc., Chem. Commun. (1985) 56.
[11] B.P. Sullivan, T.J. Meyer, J. Chem. Soc., Chem. Commun. (1984) 1244.
[12] J.M. Kelly, J.G. Vos, Angew. Chem., Int. Ed. Engl. 21 (1982) 628.
[13] J.G. Haasnoot, W. Hinrichs, O. Weir, J.G. Vos, Inorg. Chem. 25 (1986) 4140.
[14] D.J. Cole-Hamilton, J. Chem. Soc., Chem. Commun. (1980) 1213.
[15] P.G. Jessop, T. Ikariya, R. Noyori, Chem. Rev. 95 (1995) 259.
[16] D.A. Palmer, R.V. Eldik, Chem. Rev. 83 (1983) 651.
[17] D.J. Darensbourg, R.A. Kudaroski, Adv. Organomet. Chem. 22 (1983) 129.
[18] S. Inoue, N. Yamazaki, Organic and Bioorganic Chemistry of Carbon Dioxide, Kodansha, Tokyo, 1981.
[19] M.E. Vol'pin, I.S. Kolomnikov, Pure Appl. Chem. 33 (1975) 567.
[20] K. Kalyanasundaram, M. Grätzel (Eds.), Photosensitization and Photocatalysis using Inorganic and Organometallic Compounds, Kluwer, Dordrecht, 1993.
[21] K. Kalyanasundaram, Photochemistry of Polypyridine and Porphyrin Complexes, Academic Press, London, 1992.
[22] O. Ishitani, N. Inoue, K. Koike, T. Ibusuki, J. Chem. Soc., Chem. Commun. (1994) 367.
[23] H. Ishida, T. Terada, K. Tanaka, T. Tanaka, Inorg. Chem. 29 (1990) 905.
[24] M.M. Ali, H. Sato, T. Mizukawa, K. Tsuge, M. Haga, K. Tanaka, Chem. Commun. (1998) 249.
[25] T. Inui, M. Anpo, K. Izui, S. Yanagida, T. Yamaguchi (Eds.), Advance in Chemical Conversions for Mitigating Carbon Dioxide, Elsevier, Amsterdam, 1997, p. 219.
[26] S. Chardon-Noblat, A. Deronzier, R. Ziessel, D. Zsoldos, Inorg. Chem. 36 (1997) 5384.
[27] H. Nagao, T. Mizukawa, K. Tanaka, Inorg. Chem. 33 (1994) 3415.
[28] T. Mizukawa, K. Tsuge, H. Nakajima, K. Tanaka, Angew. Chem., Int. Ed. Engl. 38 (1999) 362.
[29] J.M. Kelly, J.G. Vos, J. Chem. Soc., Dalton Trans. (1986) 1045.
[30] P. Homanen, M. Haukka, T.A. Pakkanen, J. Pursiainen, R.H. Laitinen, Organometallics 15 (1996) 4081.
[31] H. Hori, J. Ishihara, K. Koike, K. Takeuchi, T. Ibusuki, O. Ishitani, Chem. Lett. (1997) 273.
[32] S.C. Rasmussen, S.E. Ronco, D.A. Mlsna, M.A. Billadeau, W.T. Pennington, J.W. Koils, J.D. Petersen, Inorg. Chem. 34 (1995) 821.
[33] G. Maerker, F.H. Case, J. Am. Chem. Soc. 80 (1958) 2745.
[34] A. Altomare, G. Cascarano, C. Giacovazzo, A. Guagliardi, M.C. Burla, G. Polidori, M. Camalli, J. Appl. Crystallogr. 27 (1994) 435.
[35] C. Edwards, C.J. Gilmore, S. Mackey, N. Stewart, CRYSTANGM, Version 6.3.3, Program for the Solution and Refinement of Crystal Structures, Mac Science, Japan, 1996.
[36] J.A. Ibers, W.C. Hamilton (Eds.), International Tables for X-ray Crystallography, vol. IV, Kynoch Press, Birmingham, UK, 1974.
[37] E. Fujita, D.J. Szalda, C. Creutz, N. Sutin, J. Am. Chem. Soc. 110 (1988) 4870.

[38] M.H. Schmidt, G.M. Miskelly, N.S. Lewis, J. Am. Chem. Soc. 112 (1990) 3420.
[39] K. Nakamoto, Infrared and Raman Spectra of Inorganic and Coordination Compounds, fifth edn., Wiley, New York, 1997.
[40] U. Mayer, V. Gutmann, W. Gerger, Monatsh. Chem. 106 (1975) 1235.
[41] V. Gutmann, E. Wychera, Inorg. Nucl. Chem. Lett. 2 (1966) 257.
[42] R.C. Weast, D.R. Lide, M.J. Astle, W.H. Beyer (Eds.), CRC Handbook of Chemistry and Physics, 70th edn., CRC Press, Boca Raton, FL, 1990.
[43] H. Konno, K. Sakamoto, O. Ishitani, unpublished results.
[44] M.Y. Darensbourg, C.E. Ash, Adv. Organomet. Chem. 27 (1987) 1.
[45] J.H. Merrifield, J.A. Gladysz, Organometallics 2 (1983) 782 and Refs. therein.
[46] J. Guilhem, C. Pascard, J.-M. Lehn, R. Ziessel, J. Chem. Soc., Dalton Trans. (1989) 1449.
[47] H. Nagao, N. Nagao, D. Ooyama, Y. Sato, T. Oosawa, H. Kuroda, F.S. Howell, Chem. Lett. (1998) 473.
[48] M.K. Whittlesey, R.N. Perutz, M.H. Moore, Organometallics 15 (1996) 5166.
[49] L.K. Fong, J.R. Fox, N.J. Cooper, Organometallics 6 (1987) 223.
[50] D.J. Darensbourg, M. Pala, J. Am. Chem. Soc. 107 (1985) 5687.
[51] C. Bianchini, C.A. Ghilardi, A. Meli, S. Midollini, Inorg. Chem. 24 (1985) 924.
[52] D.M. Grove, G. van Koten, H.C.J. Ubbels, R. Zoet, A.L. Spek, J. Organomet. Chem. 263 (1984) C10.
[53] D.J. Darensbourg, M.B. Fischer, R.E. Schmidt, B.J. Baldwin, J. Am. Chem. Soc. 103 (1981) 1297.
[54] A. Immirzi, A. Musco, Inorg. Chim. Acta 22 (1977) L35.
[55] M.A. Billadeau, W.T. Pennington, J.D. Petersen, Acta Crystallogr., Sect. C 46 (1990) 1105.
[56] C.R. Hecker, P.E. Fanwick, D.R. McMillin, Inorg. Chem. 30 (1991) 659.
[57] D.J. Szalda, F. Fagalde, N.E. Katz, Acta Crystallogr., Sect. C 52 (1996) 3013.